

## **Strength evolution of ice plume deposit analogs of Enceladus and Europa**

*M. Choukroun<sup>1</sup>, J.L. Molaro<sup>1,2</sup>, R. Hodyss<sup>1</sup>, E. Marteau<sup>1</sup>, P. Backes<sup>1</sup>, E.M. Carey<sup>1</sup>, W. Dhaouadi<sup>1,3</sup>, S. Moreland<sup>1</sup>, E.M. Schulson<sup>4</sup>*

<sup>1</sup>Jet Propulsion Laboratory, California Institute of Technology, Pasadena, CA.

<sup>2</sup>Planetary Science Institute, Tucson, AZ.

<sup>3</sup>ETH Zürich, Zurich, Switzerland.

<sup>4</sup>Thayer School of Engineering, Dartmouth College, Hanover, NH.

### **Contents of this file**

Texts S1 to S2  
Figures S1 to S3  
Tables S1 to S3

### **Introduction**

This supporting information document provides clarifications on Materials and Methods (Text S1, Figures S1-S3, Tables S1-S2), the justification for discarding results obtained on one outlier sample in one experiment from the analysis (Text S2), and record of the fit parameters of the linear regressions conducted for cone penetration resistance measurements over time at each temperature, as well as corresponding errors, to reproduce the Arrhenius plot shown in Figure 2-b (Table S3).

## **Supplementary Text**

### **Text S1: Materials and Methods**

#### **1. Ice plume deposit analog preparation**

Fine-grained porous water ice samples were prepared by direct deposition of an air-atomized pure water mist into liquid nitrogen. The water (deionized, Fischer Scientific) mist was generated with an atomizing nozzle (Spraying Systems, Inc.) supplied with gaseous nitrogen at 3 bars pressure. The nozzle was held directly above a 14 L copper container filled with liquid nitrogen, and was wrapped in heating tape to prevent water from freezing inside the nozzle during sprays.

This process yields fine-grained spherules of water ice (Figure S1-a). Ice grains were held at 173 K within a liquid nitrogen-cooled optical cryostage (Linkam LTS350) and imaged in reflected illumination with an Olympus BX51 microscope equipped with an Olympus SC-30 camera (Choukroun et al., 2011). Images were processed and grains analyzed with the Olympus Stream software. The mean grain size (diameter) of the ice spherules is 12  $\mu\text{m}$ , and the grain size follows a log-normal distribution. The largest ice spherules had a diameter of 90  $\mu\text{m}$ . Ice samples were transported in liquid nitrogen, then transferred into the diffuse reflectance attachment of a Nicolet 6700 Fourier Transform Infrared Spectrometer, pre-cooled to 120 K. Infrared spectra in diffuse reflectance mode exhibit characteristic features of crystalline water ice (Figure S1-b).

#### **2. Long-term sintering and strength testing**

Samples of fine-grained porous ice aggregates (between 0.66 and 2.14 kg each) were prepared as described above, and the slush of ice and liquid nitrogen was poured into plastic containers. Boil-off of liquid nitrogen was monitored over laboratory scales and the samples held at 193 K between weight measurements. Once the liquid nitrogen had completely boiled off, the sample containers were capped and sealed, and placed within glove bags in chest freezers held at a constant temperature (193 K, 223 K, 233K, 243 K). Three to seven samples were prepared then stored for each run, and are further described in Table S1. The samples were held in these isothermal conditions (to the precision of the freezers thermostats, around +/- 1 K) over extended periods of time, between 2 and 14 months.

In a separate experiment, five 100-mL graduated cylinders were filled with the ice-LN<sub>2</sub> slush in order to measure the ice density. The cylinder samples were allowed to boil-off, then the bulk ice volume was measured and the samples weighed. The bulk density of the starting ice was determined by averaging all five sample cylinder measurements to  $0.446 \pm 0.015$  g/cc. Assuming an ice density of 0.92 g/cc, the bulk porosity of the starting ice sample was derived to  $51.5 \pm 1.6$  %. The cylinders were then sealed with Parafilm and kept at 243 K for up to 55 days. The mass of the cylinders and the volume of ice were measured a few times in this interval, showing no significant change in bulk density nor porosity (Table S2 and Figure S2).

The strength of the samples was measured multiple times over the course of the experiments using a custom-built upright cone penetrometer apparatus (Figure S3). This

apparatus used a linear actuator and potentiometer to drive a custom 1-cm diameter stainless steel cone with half-opening angle of  $30^\circ$  and recessed rod, pre-cooled in liquid nitrogen, through the samples at a speed of 1 cm/s, corresponding to a high strain rate of approximately  $1 \text{ s}^{-1}$ . The force exerted by the ice sample on the cone tip was measured with a 500-lb rated S-style load cell (Transducer Techniques LLC), whose response was calibrated by imposing a range of given input voltages and testing grill brick and cement-based porous comet simulants samples of known strength (Carey et al., 2017). The cone penetration resistance of the samples was derived from the time-resolved force divided by the  $78.5 \text{ mm}^2$  cross-section of the cone. All data were recorded using LabView.

Each cone penetration test was destructive and left behind a hole in the samples. Early in the experiments, some closure of the holes was observed. After a few weeks to months of sintering, a more rigid network was seemingly established within the ice and “scars” of the tests remained open. Cracks occasionally developed between a test location and the nearest edge of the sample container. Subsequent tests were then conducted in pristine areas of the same sample. On average, each sample could be tested up to 5-7 times before being deemed compromised.

The mass of each ice sample was measured before cone penetration test and varied by no more than 2 g ( $\sim 0.1\%$ ) over the course of the experiments, confirming that no substantial mass loss due to sublimation occurred, nor gain due to condensation or frost deposition. The ice volume has also not been observed to vary significantly, confirming no change in density or porosity as seen in the graduated cylinders test (Figure S2 and Table S2). All changes in strength during the experiments can only be attributed to redistribution of ice within the samples.

**Text S2:** Anomalous sample from 223 K experiment discarded from the analysis

In the case of the 223 K experiment, one sample (sample #8, see Table S1) exhibited an anomalously low strength, by a factor of around 2 as compared to the other three samples, throughout the sintering experiment. This was attributed to sample preparation: unlike the other three samples that follow the same linear trend, the anomalous sample was efficiently stirred after pouring the ice-LN<sub>2</sub> slush in the sample container. This may have affected the settling of ice grains in the slush and either preserved a more porous structure, or induced a vertical fractionation, with larger ice grains migrating to the top of the samples. Both effects could result in lower overall strength and slower sintering, as that process is strongly dependent on packing arrangement (Molaro et al., 2019). Although not reported in the article, these data are available as part of the entire dataset at [data.caltech.edu](http://data.caltech.edu).

**Supplementary Figures**

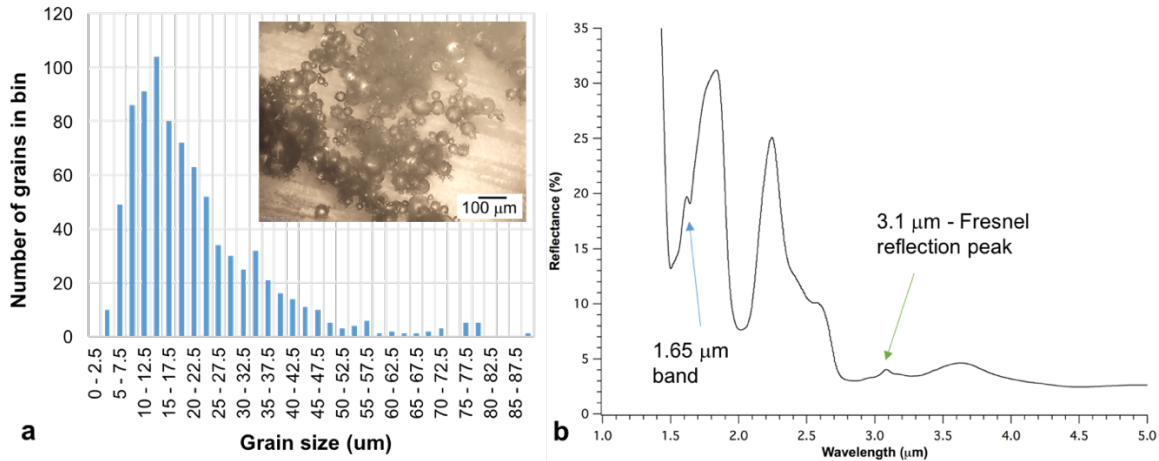


**Figure S1.** Deposition of atomized H<sub>2</sub>O into LN<sub>2</sub> produces small spherules of microcrystalline ice, with a well-constrained log-normal grain size distribution. a) Grain size distribution derived from measurements on 840 grains, and microphotograph (10x objective) obtained at 173 K of one region within the sample. b) FTIR spectrum obtained in diffuse reflectance mode with a Nicolet 6700 near- and mid-IR spectrometer at 120 K, exhibiting features that are characteristic of very fine-grained crystalline water ice (Schmitt et al., 1989).

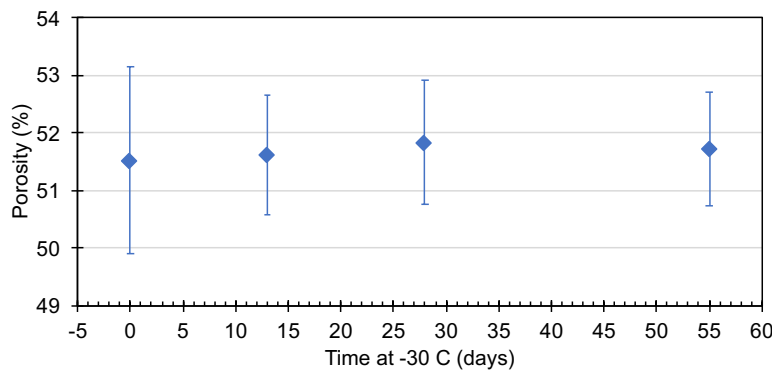


**Figure S2.** The bulk porosity of 5 ice samples sintered at 243 K show no statistically significant variation in porosity nor density over the course of the experiment, while their cone penetration resistance increased from ~ 50 kPa (starting ice) to 8-10 MPa in that time interval (Figure 2-a).

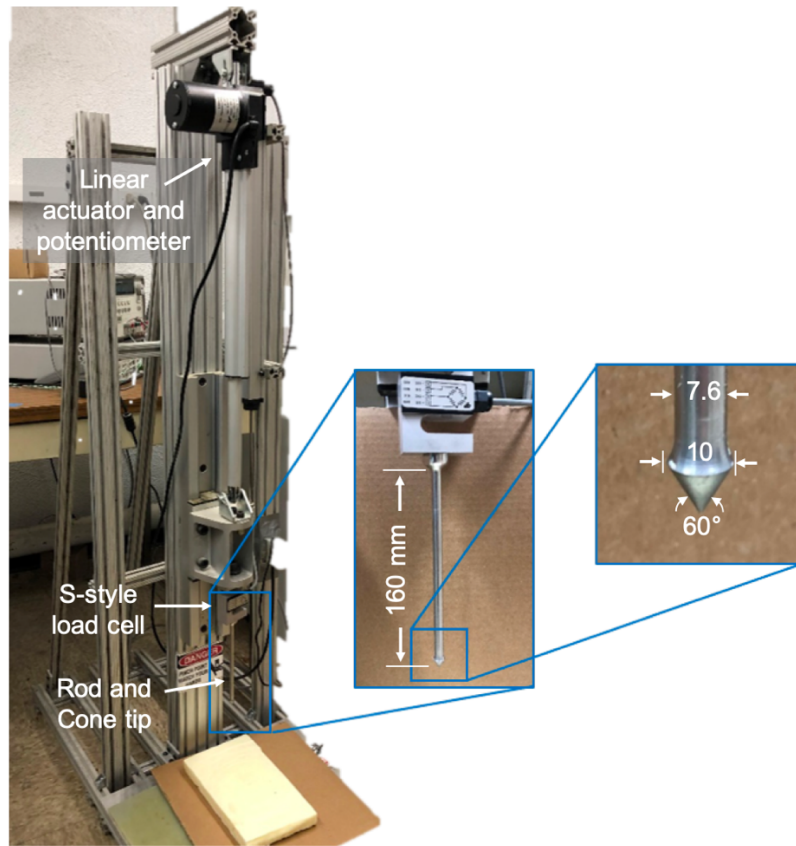


**Figure S3.** Photographs of the custom cone penetrometer apparatus used in this study. All dimensions are in mm.

**Supplementary Tables**

**Table S1.** Description of samples and sintering conditions used in this study.

Experiment	Conditions	Sample ID	Ice mass (g)	Cone penetration tests / Notes
1	193 K for 2 weeks then 243 K <sup>a</sup>	1	1134	2 (193 K) then 4 (243 K)
		2	1124	2 (193 K) then 5 (243 K)
		6	657	3 (193 K) then 3 (243 K)
		8	1177	3 (193 K) then 2 (243 K)
		10	1224	3 (193 K) then 3 (243 K)
2	223 K	8	1366	8; Anomalous sample (Text S2)
		9	2076	6
		17	2005	6
		18	2143	7
3	193 K	19	1302	4
		20	1491	2
		21	1144	3
		22	1196	3
		10	1120	3
4	233 K	1	1673	3
		2	1563	Not tested, sintering ongoing
		3	1441	3
		4	1711	3
		5	1415	1
		6	757	2
5	243 K	7	1616	2
		8	1732	Not tested, sintering ongoing
		10	1625	2
		11	1690	2
		12	1844	1
		13	2044	1
		15	1107	1

<sup>a</sup>: In this first experiment, the lack of substantial strengthening over 2 weeks at 193 K drove the decision to move samples to the warmer 243 K temperature in order to speed up sintering. In retrospect, this decision was justified, as less strengthening was observed over 2 weeks at 193 K than in 1 day at 243 K.

**Table S2.** Experimental data of density and derived porosity for the 5 graduated cylinders, averaged. The 1 $\sigma$  error is the standard deviation between all individual measurements on each day of testing.

Time (d)	Bulk density (g/cc)	1 $\sigma$ error (g/cc)	Porosity (%)	1 $\sigma$ error (%)
0	0.446	0.015	51.5	1.6
13	0.445	0.010	51.6	1.0
28	0.443	0.010	51.8	1.1
55	0.444	0.009	51.7	1.0

**Table S3.** Fit coefficient parameters from linear regression of the cone penetration resistance as function of time at each temperature, in Pascals per day (Pa/d), their  $2\sigma$  uncertainty, and their natural logarithm as represented in Figure 2-b.

Temperature (K)	Inverse Temperature ( $10^{-3} \text{ K}^{-1}$ )	Strengthening rate (Pa/d)	$2\sigma$ uncertainty (Pa/d)	Ln (best-fit rate)	Ln (best-fit - $2\sigma$ )	Ln (best-fit + $2\sigma$ )
243	4.12	$1.24 \times 10^5$	$2.96 \times 10^4$	11.73	11.46	11.95
233	4.29	$5.93 \times 10^4$	$3.63 \times 10^4$	10.99	10.04	11.47
223	4.48	$4.41 \times 10^4$	$8.26 \times 10^3$	10.69	10.49	10.89
193	5.18	$5.46 \times 10^3$	$1.28 \times 10^2$	8.60	8.37	8.79